IOP PUBLISHING PHYSICS IN MEDICINE AND BIOLOGY

Phys. Med. Biol. **55** (2010) 237–246 doi:10.1088/0031-9155/55/1/014

Complexity and accuracy of image registration methods in SPECT-guided radiation therapy

L S Yin[1,2], L Tang[3], G Hamarneh[3], B Gill[2], A Celler[4], S Shcherbinin[4], T F Fua[5], A Thompson[5], M Liu[6], C Duzenli[1,2], F Sheehan[5] and V Moiseenko[1,2]

[1] Physics and Astronomy, University of British Columbia, 6224 Agricultural Road, Vancouver, BC, V6T 1Z1, Canada
[2] Medical Physics, Vancouver Cancer Centre, BC Cancer Agency, 600 West 10th Ave, Vancouver, BC, V5Z 4E6, Canada
[3] Computing Science, Simon Fraser University, 9400 TASC1, Burnaby, BC, V5A 1S6, Canada
[4] Department of Radiology, University of British Columbia, 828 West 10th Ave, Vancouver, BC, V5Z 1L8, Canada
[5] Radiation Oncology, Vancouver Cancer Centre, BC Cancer Agency, 600 West 10th Ave, Vancouver, BC, V5Z 4E6, Canada
[6] Radiation Oncology, Fraser Valley Cancer Centre, BC Cancer Agency, 13750 9th Ave, Surrey, BC, V3V 1Z2, Canada

E-mail: lyin@bccancer.bc.ca

Received 19 August 2009, in final form 16 November 2009
Published 11 December 2009
Online at stacks.iop.org/PMB/55/237

Abstract

The use of functional imaging in radiotherapy treatment (RT) planning requires accurate co-registration of functional imaging scans to CT scans. We evaluated six methods of image registration for use in SPECT-guided radiotherapy treatment planning. Methods varied in complexity from 3D affine transform based on control points to diffeomorphic demons and level set non-rigid registration. Ten lung cancer patients underwent perfusion SPECT-scans prior to their radiotherapy. CT images from a hybrid SPECT/CT scanner were registered to a planning CT, and then the same transformation was applied to the SPECT images. According to registration evaluation measures computed based on the intensity difference between the registered CT images or based on target registration error, non-rigid registrations provided a higher degree of accuracy than rigid methods. However, due to the irregularities in some of the obtained deformation fields, warping the SPECT using these fields may result in unacceptable changes to the SPECT intensity distribution that would preclude use in RT planning. Moreover, the differences between intensity histograms in the original and registered SPECT image sets were the largest for diffeomorphic demons and level set methods. In conclusion, the use of intensity-based validation measures alone is not sufficient for SPECT/CT

registration for RTTP. It was also found that the proper evaluation of image registration requires the use of several accuracy metrics.

(Some figures in this article are in colour only in the electronic version)

1. Introduction

The objective of radiotherapy treatment planning (RTTP) is to deliver a therapeutic dose of radiation to the target, while minimizing the risk of complications due to the irradiation of normal tissues within the body. In current clinical practice, 5–20% of patients treated with radiation for intrathoracic malignancies, such as lung cancer, develop symptomatic lung complications. Currently, the radiation burden on the lungs of a patient is calculated as the volume of lung receiving more than a certain dose during therapy. A commonly used example of this is V20, wherein the percentage volume of healthy lung receiving at least 20 Gy has been found through population studies to be unlikely to cause severe radiation pneumonitis at levels less than 30% (Graham *et al* 1999).

The V20 metric is flawed in that lung volume is used as a surrogate for lung function. The inadequacy of this assumption has been demonstrated in a number of studies reporting higher incidence of radiation pneumonitis occurring in the lower half of patients' lungs compared to lung apices (Yorke *et al* 2002, Seppenwoolde *et al* 2004). Marks *et al* (1999) have demonstrated that the incorporation of perfusion single photon emission tomography (SPECT) imaging using macro-aggregated albumin (MAA) has the potential to reduce treatment-related morbidity for patients with lung cancer. The viability of this approach was shown by Seppenwoolde *et al* (2004) who reported that combining the local perfusion data with mean regional dose explained some of the differences in radiosensitivity between posterior and anterior lung. Image registration of SPECT images to RTTP images allows planners to identify sites with high or low perfusion values, and should result in plans with the lowest possible radiation burden to lung function, and therefore lowest complication rates.

Using SPECT in RTTP, however, requires careful registration of functional SPECT images with anatomical CT images that are used for therapy planning. When SPECT images are acquired using a hybrid SPECT/CT camera, this registration is relatively easier than it is in situation when only SPECT data are available, as it can employ CT-to-CT registration. In this case, the CT set acquired from a hybrid SPECT/CT scan is first registered to the RTTP CT. The same transformation and warping obtained from this registration is then applied to the SPECT images so that they too are registered to the RTTP CT. Several methods of registering images exist. Previously reported clinical studies used point-based registration and rigid registration (Christian *et al* 2005, Lavrenkov *et al* 2007, 2009) using either fiducial markers placed physically on the skin, or using anatomical and physiological landmarks that have been identified manually as corresponding pairs in both CT images. Automated non-rigid registration methods resolve a displacement field such that when it is applied to one image, the image becomes aligned with the target image. Non-rigid methods often involve a set of parameters that control the amount of regularization being enforced on the displacement field; these will affect the resulting spatial transformation or the corresponding displacement vector field. We performed initial experiments to empirically determine the values for these parameters that would allow us to successfully register our image sets, but would not restrict the transformation excessively.

In this paper, we report on the use of six registration methods to register CT images for the purpose of aligning the corresponding SPECT images to the planning CT. The

methods used vary in their complexity from the simplest rigid co-registration, to 3D affine transform based on control points placed on the skin or lung landmarks, to non-rigid registration using a B-spline transformation, or diffeomorphic demons and level set non-rigid registration. We evaluate the quality of co-registration using various validation metrics.

2. Methods

Institutional ethics approval was acquired prior to recruiting patients.

2.1. Image acquisition and reconstruction

Ten patients (six males aged: 50 ± 10 years, four females 40 ± 10 years) recently diagnosed with lung cancer and referred for radiation therapy consented to have a perfusion SPECT scan for the purpose of this study. Nine of these patients were diagnosed with non-small cell lung cancer (NSCLC) and one with small cell lung cancer (SCLC). In order to localize the tumor volume and set up radiation fields, a conventional planning CT scan was performed with patients in the treatment position: patients lay down supine on a flat bed with head rest and knee supports. Arms were raised and supported above the head. The CT scan was reconstructed to matrix size of $512 \times 512 \times 80$ voxels, each of size $0.96 \times 0.96 \times 5$ mm^3). Treatment planning and dose calculations were performed on this CT set. Thus, it was selected as the *fixed CT image* in the image registration. Radio-opaque markers were placed on the skin of each patient as a reference for subsequent SPECT/CT scans and treatments.

The perfusion SPECT scan was acquired prior to radiation therapy. The SPECT scanner bed was fitted with a flat couch top to ensure that the patients' position is consistent with the RT treatment position. The same immobilization device and arm support were used in both the SPECT scan and planning CT scan. In each case, 185 MBq of 99mTc-macroaggregated albumin (MAA) was injected intravenously. The lung perfusion scan was acquired using the Infinia-Hawkeye SPECT/CT camera (GE Healthcare) with the low-energy high-resolution (LEHR) collimator. The detectors were positioned in H-mode (relative angle 180°), the acquisition matrix was 128×128 and a total of 120 projections (60 camera stops per head) with 20 s/stop were acquired over a total of 360° camera rotation with a non-circular orbit (NCO). The perfusion SPECT image acquired from this scan (which we labeled the *moving SPECT image*) was reconstructed to a matrix of dimensions $128 \times 128 \times 128$ voxels, each $4.42 \times 4.42 \times 4.42$ mm^3. The reconstruction was performed using the ordered subsets expectation maximization (OSEM) algorithm which incorporated resolution recovery (RR) as well as corrections for attenuation and scatter (SC) (Vandervoort *et al* 2005).

The SPECT scan was followed by a low dose CT scan performed with the same SPECT/CT camera. This CT dataset (labeled *moving CT image*) was of dimensions $256 \times 256 \times 40$ voxels (each $2.21 \times 2.21 \times 10$ mm^3) and was subsequently used for creation of the patient-specific attenuation map and for planning-CT to SPECT co-registration. SPECT, planning CT and low-dose CT scans were all performed while the patient was free breathing.

2.2. Image co-registration methods

2.2.1. Skin control point-based registration ('skin method'). This method was previously used to register SPECT images from a stand-alone SPECT scanner with no CT capability (Christian *et al* 2005, Lavrenkov *et al* 2007, 2009). A set of 8–12 control points on the skin

contour was selected to resolve a 3D affine transform that minimizes the distance between the corresponding control points in a least-squares sense.

2.2.2. Lung control point-based registration ('lung method'). This method employs the same approach to find image transformation as the 'skin method'. But here, instead of selecting control points on the radio-opaque markers, these were manually located within the lung in the SPECT CT and RTTP CT scans.

2.2.3. Rigid registration ('rigid'). The *fixed CT image* and *moving CT image* were transformed rigidly to minimize the negative value of the mutual information (MI) metric between the two images (Mattes *et al* 2001). A regular step gradient descent optimizer was used to drive the optimization with maximum step length 0.15, minimum step length 5×10^{-6} and 200 iterations.

2.2.4. B-spline non-rigid registration ('B-spline'). We employed a gradient-descent-based optimizer to resolve the parameters of a B-spline transform that minimizes the negative value of the MI metric as in rigid registration. The combined use of B-spline regularization and MI was found to be suitable for CT lung registration by De Craene *et al* (2006). Two levels of registration were used with the first and second levels using 15 and 34 nodes on the B-spline grid respectively.

2.2.5. Diffeomorphic demons non-rigid registration ('demons'). This is an optical-flow-like technique which has been applied to lung CT registration by Wang *et al* (2005). We used the diffeomorphic version of this technique as done by Vercauteren *et al* (2007), which ensures that the computed transformation has a differentiable inverse so that the topology of anatomical structures is preserved after registration. Two levels of registration were used with 25 iterations in each level. Maximum update step length was set to 2.

2.2.6. Level set non-rigid registration ('level set'). This method is in essence a more efficient and computationally faster version of the demons method, wherein a level-set model is used to model deformations (Vemuri *et al* 2000). Two levels of registration were used with 25 iterations in each level. The deformation field was smoothed with a smoothing kernel (standard deviation set to 2) during the iterations.

2.3. Registration evaluations

The results for CT–CT registration can be evaluated qualitatively or quantitatively using different figures of merit. The success of registration for our purposes also requires that the deformation field, when applied to the SPECT images, creates valid (clinically realistic and acceptable for use in therapy planning) images. For non-rigid registration, if the regularization on the displacement field is insufficient, folding and discontinuities may result in the generated displacement field (e.g. displacement vectors of two adjacent voxels may cross over each other) such that applying them to SPECT images would yield false or implausible activity counts or activity distributions.

A common quantitative assessment of image registration is to calculate the target registration error (TRE) using two sets of corresponding landmarks identified in the registered images by clinical experts (Fitzpatrick *et al* 1998). This approach is not suitable for lung images, however, as reproducible identification of landmarks in lung is difficult. A variety of automatic image registration metrics (Wang *et al* 2005, Vemuri *et al* 2000, Urschler *et al*

2007) can be calculated from a registered image pairs; these include: $\mathrm{RMS}_{\mathrm{int}}$—the root mean square of intensity differences, $\mathrm{MAD}_{\mathrm{int}}$—median-absolute deviation of intensity differences, and $\mathrm{MID}_{\mathrm{int}}$—maximum intensity differences. The corresponding equations for $\mathrm{RMS}_{\mathrm{int}}$ and $\mathrm{MAD}_{\mathrm{int}}$ are

$$\mathrm{RMS}_{\mathrm{int}} = \sqrt{\frac{1}{N}\left(I_F(x) - I_M(x)\right)^2} \tag{1}$$

$$\mathrm{MAD}_{\mathrm{int}} = \mathrm{Median}(|d(x) - \mathrm{Median}(d(x))|) \tag{2}$$

where $I_F(x)$ and $I_M(x)$ are fixed and moving CT image intensities, respectively; $d(x) = I_F(x) - I_M(x)$.

In our analysis, the maximum intensity difference was defined as the intensity difference which was larger than 95% of all differences. For simplicity, we shall now refer to $\mathrm{RMS}_{\mathrm{int}}$, $\mathrm{MAD}_{\mathrm{int}}$ and $\mathrm{MID}_{\mathrm{int}}$ collectively as intensity-based measures. While these metrics may reflect the success of the optimization procedure in registering the images, they unfortunately do not assess the validity of the deformations computed by the algorithms, as will be shown in section 3.

Qualitative validation involves the use of individual experts to assess image registration through the use of difference images, or display tools such as image overlays. This method suffers from a lack of a quantifiable metric to rank the quality of a given registration, and like the calculated metrics, cannot clearly reflect the validity of the deformation fields. After the completion of image registration, two radiation oncologists identified reference points on selected anatomical and physiological landmarks (e.g. the most anterior, lateral and posterior extent of lung parenchyma, the junctions of the anterior and posterior mediastinum with chest wall and most lateral extent of mediastinal contour within each hemi-thorax) on the RTTP CT and registered CT sets in a double-blind study. The TRE was then calculated as the average distance between locations of these reference points as placed by radiation oncologists in the two CT sets.

Evaluation of SPECT-RTTP CT registration validity requires an additional assessment step. Since CT images are used as input images in the registrations, CT registrations were performed to preserve count density. However, we found that after the SPECT images were deformed and differences in voxel sizes were corrected, the difference in total SPECT counts before/after registration was small (within 3%). As commonly used in SPECT-guided treatment planning studies (Lavrenkov *et al* 2007, 2009), functional volume was usually segmented using a certain SPECT intensity as a threshold. Thus, we compared the difference in the functional volume of SPECT images before and after registration through the use of activity histograms. The intensity histograms of the original SPECT and the registered SPECT images were calculated in voxels with more than 10% of maximum SPECT intensities. Then, we calculated the histogram difference of the SPECT intensities ($\mathrm{HIST}_{\mathrm{SPECT}}$) as the sum of absolute volume (instead of number of voxels to account for difference in voxel sizes) difference in each bin:

$$\mathrm{HIST}_{\mathrm{SPECT}} = \sum_i \left| V^i_{\mathrm{moving}} - V^i_{\mathrm{registered}} \right| \tag{3}$$

where V^i_{moving} and $V^i_{\mathrm{registered}}$ are the volume of the ith bin in the intensity histogram of the original and registered SPECT image sets, respectively. We adopted this metric to quantify the change seen in the SPECT image after application of the transformation. Although a small value of this metric does not necessarily suggest a good registration, a large value does indicate that a substantial part of the SPECT activity distribution has been affected by registration.

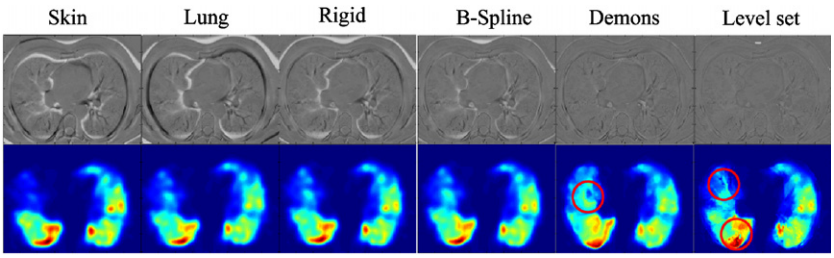

Figure 1. Above: slices of the difference image computed between the *moving CT image* and the *fixed CT image* after each registration. Below: slices of the SPECT images warped with the deformation field from each registration. Circles indicated where SPECT signals are clinically invalid.

Table 1. Averaged results of the metrics used in this study.

	Skin	Lung	Rigid	B-Spline	Demons	Level set
RMS_{int} (HU)	230.77	205.60	158.01	123.39	79.68	63.68
MAD_{int} (HU)	44.5	40.3	34	29.1	19.2	16.9
MID_{int} (HU)	577.4	507.5	358.5	258	167.9	110.5
TRE (mm)	5.629	3.8065	3.2765	1.902	1.116	0.684
$HIST_{SPECT}$ (mm^3)	7225	7832	6444	9594	18 572	15 483
JAC_{disp} (%)	0	0	0	0.2571	37.88	24.69

We also scrutinized the spatial transformations to assess the plausibility of the deformation. The determinant of the Jacobian of the displacement field gives information about local volume changes. It is defined as the determinant of the first partial derivatives of the transformation. Negative Jacobian values resemble inconsistent transformation, i.e. singularities or foldings. To assess the amount of singularities in the deformation field, we computed JAC_{disp}, the percentage of negative values in the Jacobian determinant, as done in Urschler *et al* (2007). Ideally this measure should be 0.

3. Results

The results of the six registration methods which were tested in this study, averaged over ten patients, are shown in table 1. We can see a marked improvement in the intensity-based measures from manually placed control points to automatic rigid registration, and the same trend again can be seen for automated rigid to nonlinear registration. The reduction in image differences is consistent with the reduction of TRE based on experts' review (table 1). However, based on visual examination of the registered SPECT images, we found that those generated from level set and demons registrations were not clinically realistic. Examples are shown in figure 1 where false SPECT counts (local maxima in intensity values in highlighted regions) can be seen. This was largely due to singularities (folding, etc) in the deformation field (figure 2). We also examined the level of preservation in the activity distribution in the registered SPECT images; values of the SPECT-based metric are reported in table 1 as $HIST_{SPECT}$. The average values of selected CT-based and SPECT-based metrics were normalized to the same scale and are shown in figure 3. CT-based and SPECT-based metrics increase in opposite directions. This suggests that, while the use of non-rigid registration

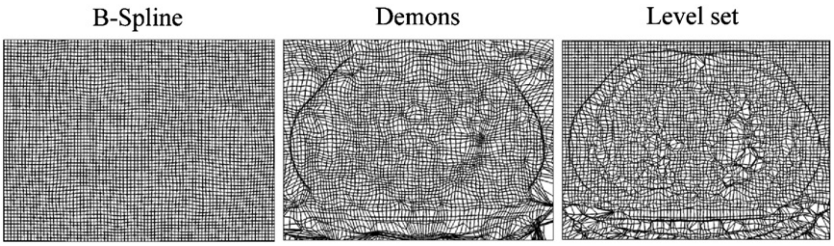

Figure 2. Slices of the deformation fields obtained from B-spline, demons and level set registrations. These slices correspond to those shown in figure 1.

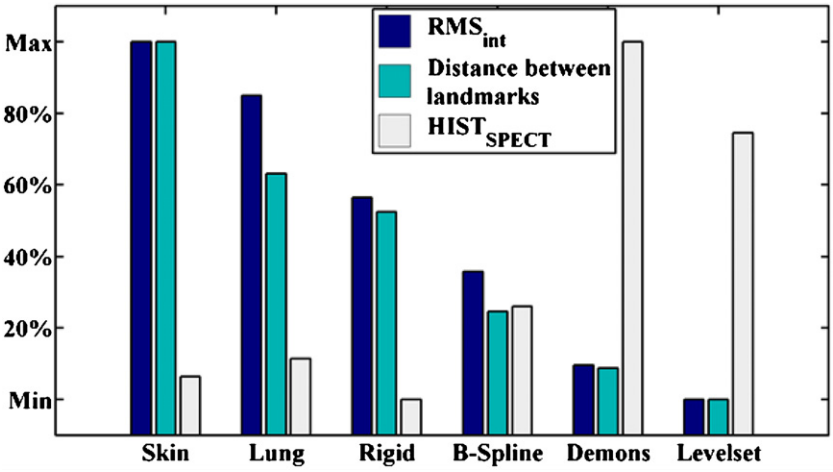

Figure 3. Renormalized average values of selected CT-based and SPECT-based metrics.

may result in improved alignment between registered CT images, the resolved deformations as obtained by the demons and level set registration algorithms actually did not result in valid registered SPECT images.

4. Discussions and conclusions

In this study, we compared the accuracies of six CT–CT registration methods, three of which are linear registration methods that have been previously reported (Christian *et al* 2005, Lavrenkov *et al* 2007, 2009, McGuire *et al* 2006, Shioyama *et al* 2007). Of these three linear registration methods, rigid (which is based on the mutual information computed from the intensities of both images and not based on manually defined point correspondences) was demonstrated to perform the best based on intensity metrics and anatomical landmarks. In the two control point-based registration methods, the skin method was found to be inferior to the lung method. This suggests that control points identified on anatomical landmarks in lungs provide better information for correct registration than those defined on the skin markers. We further introduced the use of three automated, non-rigid registration methods (B-spline, demons and level set) for image registration in SPECT-guided RT. Improvements in both the

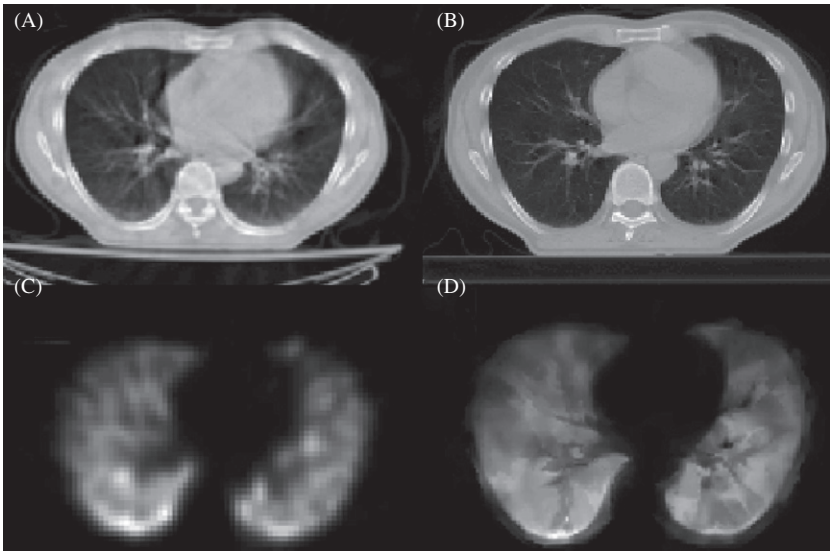

Figure 4. A sample of transversal slice in CT (A: *moving CT image*. B: *fixed CT image*) and SPECT images (C: *moving SPECT image.* D: *registered SPECT image* from level set registration). Invalid SPECT counts can clearly be seen in gray scale.

image intensity-based metrics and TRE-based metrics were observed in all three the non-rigid methods.

However, upon applying the deformation field obtained from demons and level set to the perfusion SPECT, it was determined that the activity distributions in the SPECT images were unacceptably altered. This is likely related to several factors outside the registration algorithm itself. First of all, it is known that the quality of CT images from an SPECT/CT camera is not as good as the conventional CT images. The artifacts as well as noise may have impacted the robustness of the registration algorithms in such a way that they also correct for these artifacts and noise (figure 4), thus producing invalid deformation fields and warped SPECT images. Meanwhile, a typical planning CT scan takes several minutes, whereas SPECT and subsequent CT scans can take more than half an hour. All the participating patients had lung cancer and poor lung function; however, we did not make any additional efforts to allow for patients' comfort during the scans. Consequently, breathing motions during these scans, which are not accounted for or modeled by the non-rigid registration algorithms, may have also been sources of error in registrations.

Neither intensity-based metrics nor TRE-based metrics reflected the problem of invalid deformation field in deformable registrations. This suggests that the use of metrics derived from CT image sets alone (i.e. based on control points or image similarity) do not adequately reflect the quality or accuracy of the actual registrations. Consequently, in lieu of manually inspecting the obtained displacement fields and registered SPECT images, calculation of the JAC_{disp} and $HIST_{SPECT}$ measures served as a useful 'sanity check' on the registration solutions. We draw two important conclusions here: (i) when applying the deformation parameters obtained from registration of CT to CT, it is valuable to examine how the SPECT image will be deformed. (ii) Controlling the smoothness of the displacement vector field by setting the regularization parameter is an important issue that can be crucial in deciding whether the resulting SPECT image is valid or not.

In future work, the non-rigid registration algorithms will be modified so as to explicitly enforce volume preservation (positive Jacobian), as proposed in Noblet *et al* (2004), and the preservation of SPECT count distributions. Further, we are currently exploring approaches for automatically setting the regularization parameters either based on training data or quantifying image reliability as in McInotosh and Hamarneh (2007), McInotosh and Hamarneh (2009) and Rao *et al* (2009).

While this study focused on deformable co-registration for the purpose of registering SPECT images to the planning CT, the results have broader implications. Deformable co-registration is becoming a common feature of treatment planning systems and adaptive radiation therapy (ART). Properly implemented ART requires that doses to normal tissues and target volumes be tracked through treatment on a voxel-by-voxel basis (Castadot *et al* 2008). Imaging modalities such as daily MVCT used in tomotherapy can be used for the purpose of daily image acquisitions (Lu *et al* 2006). Currently published deformable co-registration studies have emphasized a need for daily MVCT pre-processing (Yang *et al* 2009), and for the evaluation of co-registration accuracy using metrics similar to those used in this study, as well as visual examination of delineated contours. In this study, we had the benefit of inspecting the accuracy of co-registration by comparing pre- and post-warp SPECT intensity distributions in lung. We showed that certain quantitative evaluation methods of CT–CT co-registration have ranked the demons and level set methods as the best even though subjective evaluations of the deformed SPECT images did not indicate so. This applies to both metrics based on Hounsfield Units and calculations of TRE. The latter is seen as a definitive clinical validation. This is unfortunate because our experimental results have clearly shown that these measures are insufficient for validation purposes. We conclude that clinical implementation of ART should also incorporate subjective evaluations of registration results by oncologists, therapists, or physicists before treatment plan adaptations are made.

References

Castadot P, Lee J A, Parraga A, Geets X, Macq B and Gregoire V 2008 Comparison of 12 deformable registration strategies in adaptive radiation therapy for the treatment of head and neck tumors *Radiother. Oncol.* **89** 1–12

Christian J A, Partridge M, Nioutsikou E, Cook G, McNair H A, Cronin B, Courbon F, Bedford J L and Brada M 2005 The incorporation of SPECT functional lung imaging into inverse radiotherapy planning for non-small cell lung cancer *Radiother. Oncol.* **77** 271–7

De Craene M, Du Bois d'Aische A, Macq B and Warfield S K 2006 Incorporating metric flows and sparse Jacobian transformations in ITK *Insight J.* http://hdl.handle.net/1926/183

Fitzpatrick J M, Hill D L, Shyr Y, West J, Studholme C and Maurer C R Jr 1998 Visual assessment of the accuracy of retrospective registration of MR and CT images of the brain *IEEE Trans. Med. Imag.* **17** 571–85

Graham M V, Purdy J A, Emami B, Harms W, Bosch W, Lockett M A and Perez C A 1999 Clinical dose–volume histogram analysis for pneumonitis after 3D treatment for non-small cell lung cancer (NSCLC) *Int. J. Radiat. Oncol. Biol. Phys.* **45** 323–9

Lavrenkov K, Christian J A, Partridge M, Niotsikou E, Cook G, Parker M, Bedford J L and Brada M 2007 A potential to reduce pulmonary toxicity: the use of perfusion SPECT with IMRT for functional lung avoidance in radiotherapy of non-small cell lung cancer *Radiother. Oncol.* **83** 156–62

Lavrenkov K, Singh S, Christian J A, Partridge M, Nioutsikou E, Cook G, Bedford J L and Brada M 2009 Effective avoidance of a functional SPECT-perfused lung using intensity modulated radiotherapy (IMRT) for non-small cell lung cancer (NSCLC): an update of a planning study *Radiother. Oncol.* **91** 349–52

Lu W, Olivera G H, Chen Q, Ruchala K J, Haimerl J, Meeks S L, Langen K M and Kupelian P A 2006 Deformable registration of the planning image (kVCT) and the daily images (MVCT) for adaptive radiation therapy *Phys. Med. Biol.* **51** 4357–74

Marks L B, Sherouse G W, Munley M T, Bentel G C and Spencer D P 1999 Incorporation of functional status into dose–volume analysis *Med. Phys.* **26** 196–9

Mattes D, Haynor D R, Vesselle H, Lewellen T K and Eubank W 2001 Non-rigid multimodality image registration *Medical Imaging 2001: Image Processing* pp 1609–20

McGuire S M, Zhou S, Marks L B, Dewhirst M, Yin F F and Das S K 2006 A methodology for using SPECT to reduce intensity-modulated radiation therapy (IMRT) dose to functioning lung *Int. J. Radiat. Oncol. Biol. Phys.* **66** 1543–52

McInotosh C and Hamarneh G 2007 Is a single energy functional sufficient? Adaptive energy functionals and automatic initialization *Medical Image Computing and Computer-Assisted Intervention (MICCAI) (Lecture Notes in Computer Science)* pp 503–10

McInotosh C and Hamarneh G 2009 Optimal weights for convex functionals in medical image segmentation *Int. Symp. on Visual Computing: Special Track on Optimization for Vision, Graphics and Medical Imaging: Theory and Applications (ISVC OVGMI)* vol 5875-I pp 1079–88

Noblet V, Heinrich C, Heitz F and Armspach J 2004 A topology preserving non-rigid registration method using a symmetric similarity function—application to 3D brain images *Computer Vision—ECCV 2004 (Lecture Notes in Computer Science)* pp 546–57

Rao J, Hamarneh G and Abugharbieh R 2009 Adaptive contextual energy parameterization for automated image segmentation *Int. Symp. on Visual Computing: Special Track on Optimization for Vision, Graphics and Medical Imaging (ISVC OVGMI)* vol 5875-I pp 1089–100

Seppenwoolde Y, De Jaeger K, Boersma L J, Belderbos J S and Lebesque J V 2004 Regional differences in lung radiosensitivity after radiotherapy for non-small-cell lung cancer *Int. J. Radiat. Oncol. Biol. Phys.* **60** 748–58

Shioyama Y *et al* 2007 Preserving functional lung using perfusion imaging and intensity-modulated radiation therapy for advanced-stage non-small cell lung cancer *Int. J. Radiat. Oncol. Biol. Phys.* **68** 1349–58

Urschler M, Kluckner S and Bischof H 2007 A framework for comparison and evaluation of nonlinear intra-subject image registration algorithms *Insight J.* http://hdl.handle.net/1926/561

Vandervoort E J, Celler A, Wells R G, Blinder S, Dixon K L and Pang Y 2005 Implementation of an analytically based scatter correction in SPECT reconstructions *IEEE Trans. Nucl. Sci.* **52** 642–53

Vemuri B C, Ye J, Chen Y and Leonard C M 2000 A level-set based approach to image registration *IEEE Workshop on Mathematical Methods in Biomedical Image Analysis* (New York: IEEE Press) pp 86–93

Vercauteren T, Pennec X, Perchant A and Ayache N 2007 Diffeomorphic demons using ITK's finite difference solver hierarchy *Insight J.* http://hdl.handle.net/1926/510

Wang H, Dong L, O'Daniel J, Mohan R, Garden A S, Ang K K, Kuban D A, Bonnen M, Chang J Y and Cheung R 2005 Validation of an accelerated 'demons' algorithm for deformable image registration in radiation therapy *Phys. Med. Biol.* **50** 2887–905

Yang D, Chaudhari S R, Goddu S M, Pratt D, Khullar D, Deasy J O and El Naqa I 2009 Deformable registration of abdominal kilovoltage treatment planning CT and tomotherapy daily megavoltage CT for treatment adaptation *Med. Phys.* **36** 329–38

Yorke E D, Jackson A, Rosenzweig K E, Merrick S A, Gabrys D, Venkatraman E S, Burman C M, Leibel S A and Ling C C 2002 Dose–volume factors contributing to the incidence of radiation pneumonitis in non-small-cell lung cancer patients treated with three-dimensional conformal radiation therapy *Int. J. Radiat. Oncol. Biol. Phys.* **54** 329–39